BIOCHEMISTRY
including biophysical chemistry & molecular biology

ARTICLE

pubs.acs.org/biochemistry

Identification of Immunoreactive Regions of Homology between Soluble Epidermal Growth Factor Receptor and α5-Integrin

Jason A. Wilken,[†] Andre T. Baron,[‡] Ramsey A. Foty,[§] Daniel J. McCormick,[∥] and Nita J. Maihle[*,†,⊥]

[†]Department of Obstetrics, Gynecology, and Reproductive Science, Yale School of Medicine, P.O. Box 208063, 310 Cedar Street, New Haven, Connecticut 06520-8063, United States

[‡]Department of Epidemiology, College of Public Health, and Department of Obstetrics and Gynecology, Division of Gynecologic Oncology, Lucille P. Markey Cancer Center, University of Kentucky, 800 Rose Street, Roach Building, Room CC 408, Lexington, Kentucky 40356-0093, United States

[§]Department of Surgery, University of Medicine and Dentistry of New Jersey, CAB 7070, 125 Paterson Street, New Brunswick, New Jersey 08903, United States

[∥]Department of Biochemistry and Molecular Biology, Mayo Clinic, 200 First Street Southwest, Rochester, Minnesota 55905, United States

[⊥]Departments of Pathology and Pharmacology, Yale School of Medicine, P.O. Box 208063, 310 Cedar Street, New Haven, Connecticut 06520-8063, United States

Supporting Information

ABSTRACT: Proteins encoded by the epidermal growth factor receptor (*EGFR/HER1/ERBB1*) gene are being studied as diagnostic, prognostic, and theragnostic biomarkers for numerous human cancers. The clinical application of these tissue/tumor biomarkers has been limited, in part, by discordant results observed for epidermal growth factor receptor (EGFR) expression using different immunological reagents. Previous studies have used EGFR-directed antibodies that cannot distinguish between full-length and soluble EGFR (sEGFR) expression. We have generated and characterized an anti-sEGFR polyclonal antiserum directed against a 31-mer peptide (residues 604−634) located within the unique 78-amino acid carboxy-terminal sequence of sEGFR. Here, we use this antibody to demonstrate that sEGFR is coexpressed with EGFR in a number of carcinoma-derived cell lines. In addition, we show that a second protein of ∼140 kDa (p140) also is detected by this antibody. Rigorous biochemical characterization identifies this second protein to be α5-integrin. We show that a 26-amino acid peptide in the calf domain of α5-integrin (residues 710−735) is 35% identical in sequence with a 31-mer carboxy-terminal sEGFR peptide and exhibits an approximately 5-fold lower affinity for anti-sEGFR than the homologous 31-mer sEGFR peptide does. We conclude that the carboxy terminus of sEGFR and the calf-1 domain of α5-integrin share a region of sequence identity, which results in their mutual immunological reactivity with anti-sEGFR. We also demonstrate that anti-sEGFR promotes three-dimensional tissue cohesion and compaction in vitro, further suggesting a functional link between sEGFR and α5-integrin and a role of the calf-1 domain in cell adhesion. These results have implications for the study of both EGFR and sEGFR as cancer biomarkers and also provide new insight into the mechanisms of interaction between cell surface EGFR isoforms and integrins in complex processes such as cell adhesion and survival signaling.

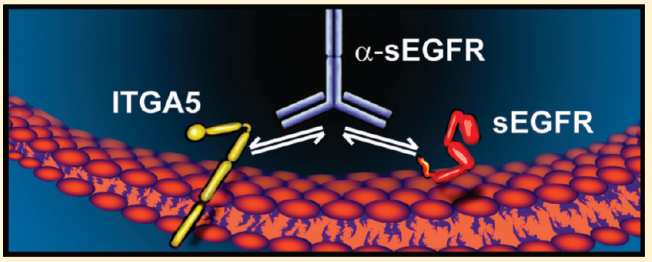

The EGFR/HER/ErbB family of receptor tyrosine kinases consists of EGFR/HER1, ErbB2/HER2/neu, ErbB3/HER3, and ErbB4/HER4. These receptors signal via both ligand-dependent[1] and ligand-independent[2] pathways to regulate cell growth, differentiation, survival, migration, and adhesion, as well as oncogenic transformation. Consequently, it is not surprising that ErbB/HER overexpression and mutational activation play major roles in the etiology and progression of human cancer. In support of this concept, a number of HER receptor-targeted therapeutics have been approved by the Food and Drug Administration (e.g., cetuximab, gefitinib, and trastuzumab) for the treatment of adult solid malignancies, while many others are under clinical investigation.[3]

EGFR is the prototypic member of the ErbB/HER receptor family; it is an ∼170 kDa glycoprotein consisting of an amino-terminal extracellular domain (ECD), a short transmembrane domain, and a carboxy-terminal intracellular domain (Figure 1). The ECD is divided into four subdomains (I−IV); subdomains I

Received: January 26, 2011
Revised: March 8, 2011
Published: April 14, 2011

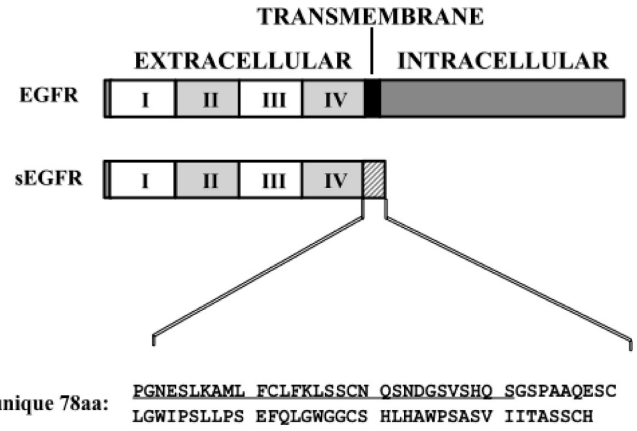

Figure 1. Schematic diagram illustrating the structure of EGFR compared to that of sEGFR. The extracellular domain is divided into four subdomains (I–IV); the transmembrane domain is indicated by the black box, and the alternate C-terminal amino acid sequence of sEGFR is indicated by the hatched box. A peptide matching the first 31 amino acids (residues 604–634) of the unique C-terminus of sEGFR (underlined) was used to generate anti-sEGFR as described by Christensen et al.[10]

and III regulate ligand binding, while subdomains II and IV regulate receptor homo- or heterodimerization. In addition to full-length EGFR, we have reported the isolation of a cDNA clone encoding a soluble EGFR isoform that contains most of the ECD but lacks the transmembrane and intracellular domains. This EGFR isoform, sEGFR, arises from an alternate splice event and incorporates a short region of novel coding sequence, including a termination codon and two polyadenylation sequences.[4] Specifically, sEGFR contains sequences encompassing EGFR ECD subdomains I–III, most of subdomain IV, and the unique 78-amino acid carboxy terminus (Figure 1).[5] This alternatively spliced sEGFR protein product is co-expressed with EGFR in diverse human tissues and also is the precursor for the major circulating isoform of EGFR in human blood, as discussed below.

While sEGFR does not contain a canonical transmembrane domain, it is, nevertheless, associated with the cell surface,[6] and we recently have shown that cell surface sEGFR is released into the extracellular milieu via a complex process that is regulated by the extracellular matrix protein fibronectin (J. A. Wilken et al., unpublished experiments). Purification of anti-EGFR reactive protein(s) from human blood reveals one major protein species that contains peptides derived from the unique carboxy terminus of sEGFR as determined by mass spectrometry.[7] Taken together, these observations support the hypothesis that sEGFR released from the cell surface enters the bloodstream via the lymphatic system and thoracic duct. Translational studies have shown that low serum sEGFR concentrations are associated with the presence of ovarian cancer,[7] poor overall survival in endometrial cancer patients,[8] and responsiveness to aromatase inhibitor therapy in breast cancer patients.[9] To develop further the clinical utility of sEGFR as a serum and tumor biomarker, we have generated polyclonal antisera directed against a 31-mer peptide (residues 604–634) located within the unique carboxy-terminal sequence of sEGFR (Figure 1).[10] This affinity-purified antibody (anti-sEGFR) is specific for sEGFR and does not detect full-length EGFR, or any other HER receptor family member.[10] Here, we report the further characterization of this anti-sEGFR antibody, including an apparent evolutionary convergence between the unique sEGFR carboxy-terminal sequence and a short bioactive sequence within the extracellular region of α5-integrin, i.e., the calf-1 domain, which coordinates ligand-dependent associations between the α and β subunits of the integrin heterodimer.[11]

MATERIALS AND METHODS

Reagents and Cell Lines. The JEG-3 choriocarcinoma cell line was purchased from American Type Culture Collection (Manassas, VA). Chinese hamster ovary (CHO) cells that stably express EGFR (CHO-EGFR), CHO cells that stably express sEGFR (CHO-sEGFR), antisera generated toward a 31-mer carboxy-terminal peptide of sEGFR (Figure 1, residues 604–634), and methods to affinity purify these polyclonal antibodies have been described previously.[10] CHO cells that express low levels of endogenous α5-integrin (CHO-B2) and CHO-B2 cells stably expressing human α5-integrin (CHO-α5) have been described previously.[12,13] CHO-P3 cells were generated by transfecting CHO-B2 cells with the pcDNA3 vector followed by G418 selection as described previously.[14] Supersignal West Femto enhanced chemiluminescent luminol (ECL) substrate, goat anti-rabbit secondary antibody, and protein A/G agarose beads were purchased from Thermo Fisher Scientific (Rockford, IL). SP Sepharose was purchased from GE Healthcare (Piscataway, NJ). Hydroxylapatite was purchased from Bio-Rad (Hercules, CA). Rabbit anti-BASP-1 (AB9306) purified antibody, α5-integrin (AB1949) antiserum, and β1-integrin (AB1952) antiserum were purchased from Millipore (Billerica, MA). Rabbit anti-EGFR (cytoplasmic domain; sc-03) purified antibody was purchased from Santa Cruz Biotechnology (Santa Cruz, CA). Rabbit IgG was purchased from Sigma (St. Louis, MO). Recombinant α5/β1 integrin and αv/β3 integrin were purchased from R&D Systems, Inc. (Minneapolis, MN). Trypsin was purchased from Promega (Madison, WI). Cyanogen bromide (CNBr, 5 M in acetonitrile) was purchased from Sigma. Peptide N-glycosidase F (PNGaseF) was purchased from New England Biolabs (Ipswich, MA).

All cell culture reagents were purchased from Mediatech (Manassas, VA), except as indicated below. A2780 and A2780 CP-R cells were maintained in RPMI-1640, supplemented with 10% fetal bovine serum (FBS), 10 μg/mL insulin, 2 mM L-glutamine, 100 units/mL penicillin, and 100 μg/mL streptomycin. ES-2 cells were maintained in McCoy's 5A medium, supplemented with 10% FBS, 2 mM L-glutamine, 100 units/mL penicillin, and 100 μg/mL streptomycin. HEY cells were maintained in DMEM/F12, supplemented with 10% FBS, 2 mM L-glutamine, 100 units/mL penicillin, and 100 μg/mL streptomycin. IGROV-1, OVCAR-5, OVCAR-8, and JEG-3 cells were maintained in DMEM supplemented with 10% FBS, 2 mM L-glutamine, 100 units/mL penicillin, and 100 μg/mL streptomycin. CHO-EGFR and CHO-sEGFR cells were maintained in F12 medium supplemented with 10% FBS, 2 mM L-glutamine, 100 units/mL penicillin, 100 μg/mL streptomycin, and 800 μg/mL G418. CHO-B2 cells were maintained in DMEM (Invitrogen, Carlsbad, CA) supplemented with 10% FBS (Hyclone, Logan, UT), 1 mM MEM nonessential amino acids, and 100 mg/mL streptomycin sulfate (Invitrogen); CHO-P3 and CHO-α5 cells were maintained in the same medium supplemented with 250 μg/mL G418.

Immunoblot Analysis of Protein Expression. Confluent or nearly confluent cells were rinsed three times with ice-cold potassium phosphate-buffered saline (K-PBS) [10 mM KH_2PO_4/K_2HPO_4 and 150 mM NaCl (pH 7.2)] and harvested by being scraped into K-PBS followed by centrifugation at 500*g* for 5 min. Cell pellets were lysed by being boiled with 2.5% sodium dodecyl sulfate (SDS), 0.5% sodium deoxycholate (DOC), and 0.5% Triton X-100 (TX-100) for 10 min. The total protein content of cell lysates was determined with a Bio-Rad DC assay. Cell lysates were boiled for 5 min with 4× Laemmli reducing buffer [0.25 M Tris (pH 6.8), 40% glycerol, 8% SDS, 2% β-mercaptoethanol, and 0.2% bromophenol blue] or 4× Laemmli nonreducing buffer (without β-mercaptoethanol), equally loaded into gel lanes based on total protein, and resolved via SDS−PAGE (7.5% acrylamide). Resolved proteins were transferred to polyvinylidene difluoride (PVDF) membrane by semidry immunoblot (Millipore), and then blocked for 1 h with Trizma-buffered saline (TBS) [10 mM Trizma and 150 mM NaCl (pH 7.4)] supplemented with 5% nonfat dry milk. Membranes were rinsed six times for 5 min each with TBS with 0.1% Tween 20 (TBS-TW20) and incubated with TBS containing 1% BSA and anti-sEGFR (168 ng/mL) or anti-EGFR (cytoplasmic domain, 50 ng/mL) overnight at 4 °C. Membranes were rinsed six times for 10 min each with TBS-TW20, incubated with goat anti-rabbit horseradish peroxidase-conjugated secondary antibody (Pierce, 2.5 ng/mL) for 1 h at room temperature, rinsed six times for 10 min each, reacted with ECL substrate, and visualized with a NucleoVISION camera station.

Purification of p140. Confluent JEG-3 cells were harvested, lysed, extracted, and subjected to cation exchange and hydroxylapatite chromatography to purify p140.

Pilot Extraction Studies. Cell pellets were lysed by boiling for 10 min in one of the following lysis solutions: (i) 2.5% SDS, 0.5% NP-40, and 0.5% DOC; (ii) 1% TX-100 and 1 mM EDTA in 10 mM Trizma (pH 7.4); (iii) 0.5% DOC; (iv) 2.5% SDS; (v) 0.5% TX-100; (vi) 0.5% DOC in TBS; (vii) 2.5% SDS in TBS; or (viii) 0.5% TX-100 in TBS. Lysates were cooled to 4 °C and centrifuged at 10000*g* for 30 min to pellet cell debris. Supernatants were assessed for p140 content by SDS−PAGE (7.5% acrylamide) and immunoblot methods.

Cation Exchange pH Optimization. Aliquots of SP Sepharose beads (0.5 mL each) were equilibrated (three washes each) with either 40 mM malonic acid (pH 2.5), 40 mM citric acid (pH 3.0 or 3.5), 100 mM formic acid (pH 4.0), 100 mM succinic acid (pH 4.5), 100 mM acetic acid (pH 5.0), 100 mM malonic acid (pH 5.5 or 6.0), 100 mM sodium phosphate (pH 7.0 or 7.5), or 100 mM HEPES (pH 8.0). JEG-3 cell lysates (0.5 mL each) prepared with unbuffered 1% TX-100 were added to each aliquot of SP Sepharose, mixed for 1 h on a rotary shaker, and briefly centrifuged to pellet the SP Sepharose. Each supernatant (100 μL) was assessed by immunoblot analysis for the binding of p140 to SP Sepharose.

Cation Exchange Chromatography. JEG-3 cell lysates prepared with unbuffered 1% TX-100 were bound to SP Sepharose equilibrated with formic acid buffer [50 mM formic acid (pH 4.0) and 0.01% TX-100] using a batch method. Unbound proteins were removed with three washes of formic acid buffer. The SP Sepharose slurry was divided into ten 0.5 mL aliquots, to which 2 M NaCl and H_2O were added to give a total volume of 1.0 mL each and final concentrations of 100, 200, 300, 400, 500, 600, 700, 800, 900, and 1000 mM NaCl. Each aliquot was mixed for 15 min on a rotary shaker, briefly centrifuged to pellet the SP Sepharose, and assessed by immunoblot analysis for p140-enriched fractions.

Hydroxylapatite Chromatography. Sodium phosphate buffer [1 M NaH_2PO_4/Na_2HPO_4 (pH 6.8)] was added to JEG-3 lysate prepared with unbuffered 1% TX-100 to give a final concentration of 20 mM sodium phosphate. Lysates were applied to a hydroxylapatite column pre-equilibrated with 20 mM sodium phosphate buffer (pH 6.8) and 0.01% TX-100 and washed with 10 column volumes of this equilibration buffer. p140 was eluted from the hydroxylapatite column with a 20 to 400 mM sodium phosphate buffer gradient.

Final Purification Scheme. JEG-3 cells were prepared with unbuffered 1% TX-100. Formic acid (1 M, pH 4.0) was added to a final concentration of 50 mM, and the solution was mixed overnight at 4 °C on a rotary shaker, followed by centrifugation at 10000*g* for 30 min to pellet precipitated protein. The supernatant was applied and eluted from a 5 mL SP Sepharose column using the buffers described above. Fractions containing p140 were pooled, adjusted to pH 6.8 with 20 mM dibasic sodium phosphate and NaOH, applied to a 5 mL hydroxylapatite column, and eluted with a 20 to 400 mM sodium phosphate buffer gradient. Fractions containing p140 were pooled, concentrated with a Speed-Vac, and analyzed by liquid chromatography and electrospray ionization tandem mass spectrometry (LC−ESI MS/MS).

Peptide Identification by LC−ESI MS/MS. Excised gel bands were washed sequentially for 5 min each with 50 mM ammonium bicarbonate and 50% acetonitrile in 50 mM ammonium bicarbonate, dehydrated with 100% acetonitrile, and rehydrated with 25 mM ammonium bicarbonate buffer containing 12.5 ng/μL trypsin. Each sample was digested at 4 °C for 1 h, decanted to remove excess solution, overlaid with 25 mM ammonium bicarbonate buffer, digested overnight at 37 °C, quenched via addition of 1 μL of 50% formic acid, and analyzed by LC−ESI MS/MS on a ThermoFinnigan LTQ linear ion trap mass spectrometer. Spectra were searched against the SwissProt database using the MASCOT (Matrix Science) search algorithm to identify the proteins of each corresponding gel band.

Miniblot Analysis of JEG-3 and HEY Lysates. JEG-3 or HEY cell lysates were loaded on a single-well gel, resolved via SDS−PAGE, and transferred to a PVDF membrane as described above. Following blocking with 5% NFDM in TBS, the PVDF membrane was placed in a miniblotter (Immunetics) and rinsed with TBS-TW20 using a vacuum manifold. Primary rabbit antibodies (65 μL per channel) directed against BASP-1, α5-integrin, β1-integrin, sEGFR, or EGFR were loaded into separate miniblotter channels and incubated for 1 h at 37 °C with gentle rocking. Each primary antibody was diluted in TBS with 1% BSA as follows: BASP-1 (1:400 to 1:1600 dilution), α5-integrin (1:400 to 1:1600 dilution), β1-integrin (1:400 to 1:1600 dilution), sEGFR (1:400 to 1:1600 dilution), and EGFR (1:200 to 1:400 dilution). The PVDF membrane was washed with TBS-TW20, incubated with secondary antibody (1:4000 dilution), and reacted with ECL reagent.

Immunoprecipitation of p140. TX-100 JEG-3 lysate was diluted 1:9 with immunoprecipitation buffer [50 mM Trizma (pH 7.4), 190 mM NaCl, 6 mM EDTA, and 2.5% TX-100] and divided into 1.2 mL aliquots. Aliquots were incubated with 1 μL of anti-α5-integrin antiserum or no antibody and mixed on a rotary shaker at 4 °C overnight. Protein A/G agarose beads (100 μL slurry) were added to each tube and mixed for an additional 3 h. The beads were rinsed three times each with immunoprecipitation wash buffer [10 mM Trizma (pH 8.3), 150 mM NaCl,

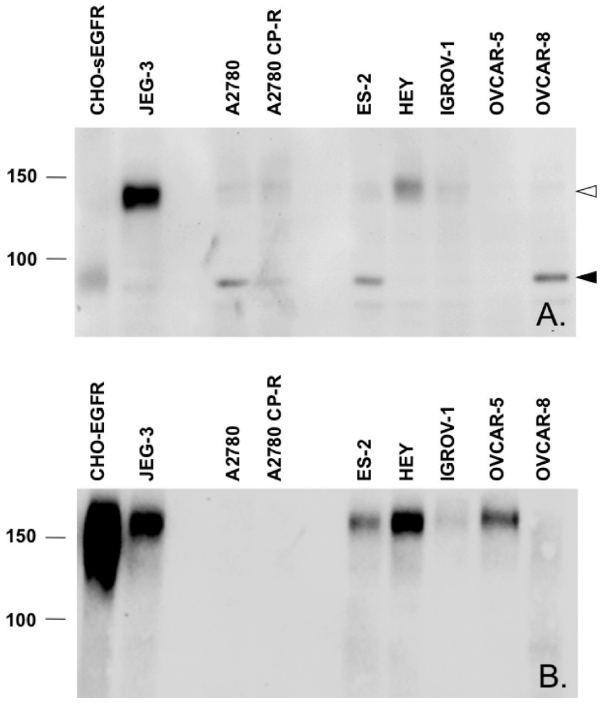

Figure 2. Expression of EGFR, sEGFR, and p140 in carcinoma-derived cell lines is detected by immunoblot analysis with anti-sEGFR. (A) An anti-sEGFR reactive band of 90 kDa, which is also reactive with a monoclonal antibody against the EGFR extracellular domain (not shown), is detected in the lysates of CHO cells stably expressing sEGFR (CHO-sEGFR), as well as in A2780, ES-2, and OVCAR-8 cells (black arrowhead). A second immunoreactive band of 140 kDa is detected in JEG-3, HEY, A2780, A2780-CP-R, ES-2, and IGROV-1 cells (white arrowhead). (B) An anti-EGFR (intracellular domain specific) reactive band of 170 kDa is detected in the lysates of CHO cells stably expressing EGFR (CHO-EGFR), as well as in JEG-3, ES-2, HEY, IGROV-1, and OVCAR-5 cells.

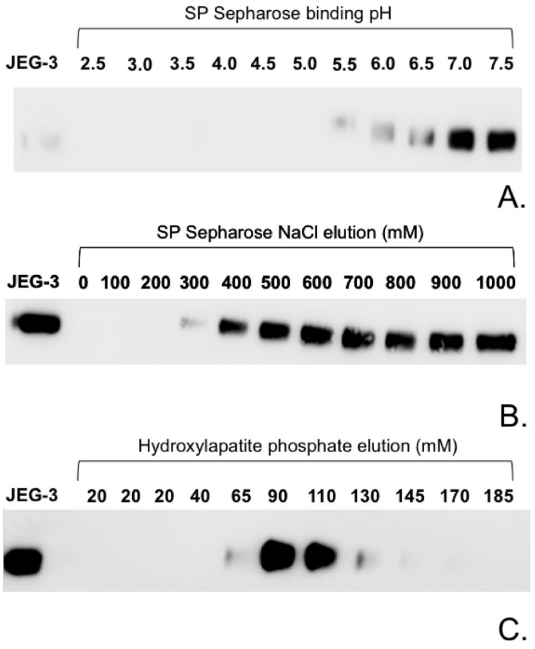

Figure 3. Chromatographic purification steps for p140 as determined by immunoblot analysis with anti-sEGFR. (A) Depletion of p140 from JEG-3 lysates with SP Sepharose at each indicated pH. After incubation of SP Sepharose at the indicated pH, supernatants were assayed for unbound p140 by immunoblot analysis with anti-sEGFR. SP Sepharose efficiently bound p140 in buffers at pH ≤5.0. (B) Elution of p140 from SP Sepharose equilibrated with 50 mM formic acid (pH 4.0) using a 0 to 1 M NaCl gradient. After incubation of SP Sepharose with cell lysates (pH 4.0) with the indicated NaCl solution, supernatants were assayed for unbound p140 by immunoblot analysis with anti-sEGFR. p140 was efficiently eluted from SP Sepharose at pH 4.0 by ≥400 mM NaCl. (C) Elution of p140 from a hydroxylapatite column equilibrated with 20 mM sodium phosphate buffer (pH 6.8) using a gradient from 20 to 185 mM sodium phosphate buffer. Eluted fractions were assayed for the presence of p140 by immunoblot analysis with anti-sEGFR. p140 was eluted from hydroxylapatite with 90−110 mM sodium phosphate (pH 6.8).

and 5 mM EDTA] and then TBS with intervening centrifugation to pellet the beads. The final protein A/G agarose pellet was boiled with 100 μL of Laemmli sample buffer for 10 min, resolved via SDS−PAGE, and processed for immunoblot analysis with anti-sEGFR.

Hydrolysis of Integrin. *CNBr.* Recombinant α5/β1-integrin in 0.05% BSA (50 μL of a 1 mg/mL stock) was lyophilized to dryness and hydrolyzed with 120 μL of a CNBr solution (70% formic acid, 15% H_2O, and 5% 5 M CNBr in acetonitrile) in the dark at room temperature. Hydrolysis was terminated via addition of 250 μL of H_2O to 20 μL of reaction solution followed by snap-freezing at 0 min, 5 min, 30 min, 1 h, 4 h, and 24 h. Samples were lyophilized and resolved on a 15% acrylamide gel via SDS−PAGE.

PNGaseF. Recombinant α5/β1-integrin in 0.05% BSA (50 μL of a 1 mg/mL stock) was denatured according to the manufacturer's instructions. Both PNGaseF-treated and untreated samples were lyophilized to dryness (note that the glycerol content of PNGaseF prevented complete lyophilization of the treated sample) and hydrolyzed with a CNBr solution for 2 h before the reaction was terminated.

Homology Alignment. Homology alignment of sEGFR residues 604−634 (31-mer) with human α5-integrin (NCBI entry NP_002196, 1008 residues) was performed using BLOSUM 62 and BLOSUM 30 alignment algorithms developed by the Genetics Computer Group (Madison, WI) and Myers and Miller.[15] Gap open and extension penalties were set to standard default values (−12 and −4, respectively) included in the program. The alignment output from both algorithms was essentially the same with the finding that BLOSUM 30 often identified longer sequence runs of residue identity. The BLOSUM 30 output indicated several regions of identity between the sEGFR 31-mer and α5-integrin, comprised of amino acid residues 637−649 (30% identical), 642−649 (38% identical), and 710−735 (35% identical). Synthetic peptides of these three homologous regions of α5-integrin and the sEGFR 31-mer were made by solid-phase peptide synthesis.

Solid-Phase Peptide Synthesis. Three human α5-integrin peptides comprising residues 637−649 (DKAQILLDCGEDN), 642−649 (LLDCGEDN), and 710−735 (PGNFSSLSCDYFAVNQSRLLVCDLGN) and an sEGFR 31-mer peptide comprising residues 604−634 (PGNESLKAMLFCLFKLSSCNQSNDGSVSHQS) were synthesized by the Peptide Synthesis Facility of the Mayo Clinic using orthogonal solid-phase methods on RINK amide resin (EMD Chemicals/Novabiochem, Gibbstown, NJ) as described previously.[16] Briefly, peptides linked to RINK resin were assembled on a Liberty Microwave Peptide Synthesizer (0.1 mmol, CEM Corp., Matthews, NC) or an APEX 396 Multiple Peptide Synthesizer (0.04 mmol,

Table 1. Summary of Amino Acid Sequences As Determined by LC−ESI MS/MS Using Fractions Enriched with p140, as Described in the Text

observed SDS−PAGE mass (kDa)	predicted m/z	ESI MS/MS protein identity	MOWSE score	peptide
140	111 kDa[a]	α5-integrin	260	120−137 LLESSLSSSEGEEPVEYK
				164−174 SLGTDLMNEMR
				695−708 VTAPPEAEYSGLVR
				760−770 TIQFDFQILSK
130	88 kDa[a]	β1-integrin	692	125−134 SGEPQTFTLK
				138−163 AEDYPIDLYYLMDLSYSMKDDLENVK
				191−202 TVMPYISTTPAK
				221−238 NVLSLTNKGEVFNELVGK
				229−238 GEVFNELVGK
				273−289 LLVFSTDAGFHFAGDGK
				326−346 LSENNIQTIFAVTEEFQPVYK
				775−784 WDTGENPIYK
				785−794 SAVTTVVNPK
52 and 130	23 kDa[a]	BASP-1	371	39−52 ESEPQAAAEPAEAK
				98−121 AEPPKAPEQEQAAPGPAAGGEAPK
				122−149 AAEAAAAPAESAAPAAGEEPSKEEGEPK
				185−198 ETPAATEAPSSTPK
				199−227 AQGPAASAEEPKPVEAPAANSDQTVTVKE

[a] α5-integrin and β1-integrin are N-glycosylated, exhibiting previously reported apparent molecular masses of ∼140 and 130 kDa, respectively, by SDS−PAGE.[36] BASP-1 migrates as an abnormally high ∼55 kDa species via SDS−PAGE.[37]

AAPPTEC, Louisville, KY) using Nα-9-fluorenyl methoxycarbonyl-protected L-amino acids and synthesis protocols provided by each instrument's manufacturer. After synthesis, peptides were cleaved in situ (Liberty synthesizer) from the resin support in a 90% trifluoroacetic acid (TFA)/5% water/5% triisopropylsilane mixture (v/v/v) for 30 min at 55 °C. Each peptide was then purified to >90% homogeneity by reverse-phase HPLC (Beckman/Coulter 126P) from a C_{18} column (Phenomonex, 2.1 cm × 25 cm) with a gradient elution of a 40% *n*-propanol/water mixture containing 0.1% TFA. The molecular mass of each HPLC-purified peptide was confirmed by electrospray ionization mass spectrometry on an MSQ single-quad instrument (Thermo Fisher Scientific), and homogeneity was assessed by analytical reverse-phase HPLC (1100 series, Agilent, Santa Clara, CA).

Peptide Quantification. The total net peptide content of each lyophilized synthetic peptide was determined by a Waters AccQ-Tag amino acid analysis method (Waters, Inc., Milford, MA). Briefly, precise dilutions of accurately weighed stock peptide solutions were prepared, and 1 μg of each stock peptide was added to a dried glass reaction vial (ashed 6 mm × 50 mm). Each peptide was hydrolyzed with 200 μL of constantly boiling HCl and a crystal of phenol at 115 °C for 20 h under a vacuum seal. The vacuum-dried samples were derivatized with 6-aminoquinolyl-*N*-hydroxysuccinimidyl carbamate according to the vendor's instructions. 6-Aminoquinolyl-derivatized amino acids were separated on a Waters AccQ-Tag column using the manufacturer's prescribed gradient on a Shimadzu 10AD HPLC system, and the integrated peak area of each amino acid was determined. Peak integration data were transferred to a Microsoft Office Excel spreadsheet, and the net peptide content was calculated using a template provided by the Association of Biomolecular Resource Facilities (http://www.abrf.org). Standard peak areas for each derivatized amino acid were determined with a known amino acid mixture (Pierce Standard H, Thermo Fisher Scientific), which was processed in parallel with the unknown peptide samples. Values for the net peptide content of each peptide were reported as the percent peptide content per milligram of dry weight.

Surface Plasmon Resonance. Binding of α5-integrin and sEGFR peptides to affinity-purified anti-sEGFR was evaluated by Precision Antibody using a Biacore 3000 surface plasmon resonance system. Briefly, goat anti-rabbit Fc was directly immobilized to a CM5 chip by amine coupling chemistry and used to capture anti-sEGFR. Binding of anti-sEGFR to α5-integrin peptide 637−649, α5-integrin peptide 710−735, and sEGFR 31-mer peptide 604−634 was first assessed by a scouting analysis (yes or no) with peptide concentrations of 200−2000 nM in assay buffer [10 mM HEPES (pH 7.4), 150 mM NaCl, 3 mM EDTA, and 0.005% polyoxyethylenesorbitan]. On the basis of first-order K_d approximation, serial 1:1 dilutions of each peptide were evaluated to calculate the equilibrium binding constant (K_D), which is the ratio of the dissociation constant (K_d) to the association constant (K_a). CM5 chips were regenerated after each assay by washing with 50 mM Trizma (pH 7.3) and 2 M NaCl.

Aggregate Compaction Assay. We have previously described methods for establishing CHO cell aggregates and quantifying CHO cell compaction.[13,17] Briefly, nearly confluent monolayers were dissociated from 10 cm tissue culture plates with trypsin/EDTA (Invitrogen). Dispersed cells were washed in complete CHO-B2 medium and centrifuged to pellet the cells. The pellet was washed with PBS and suspended in tissue culture medium containing 10% fibronectin-depleted fetal calf serum.[18] Rat plasma fibronectin was then added to the medium to a final concentration of 100 μg/mL. Cells were counted using a Bio-Rad TC10 automated cell counter and adjusted to a final concentration of 3.0×10^6 cells/mL. Aliquots (10 μL) of the cell suspension with PBS, 20 μg/mL control rabbit IgG, or 20 μg/mL anti-sEGFR were deposited on the underside of the lid of a 60 mm tissue culture dish. The bottom of the dish contained 5 mL of PBS and served to prevent evaporation of the drops by forming

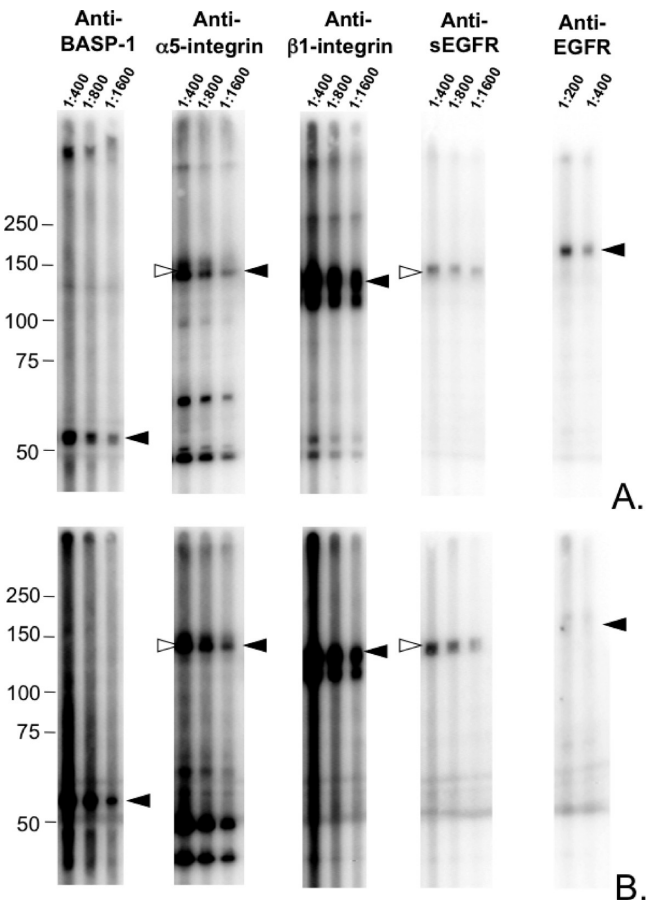

Figure 4. Expression of BASP-1, α5-integrin, and β1-intergin in JEG-3 and HEY cell lysates as detected by immunoblot analysis. JEG-3 (A) and HEY (B) cell lysates were resolved via SDS−PAGE as a single band spanning the width of the gel and transferred to a PVDF membrane. The membrane was immunoblotted using a multichannel Immentics blotter, with antibodies directed against BASP-1, α5-integrin, β1-integrin, sEGFR, and EGFR (cytoplasmic domain) at the indicated dilutions. Black arrowheads indicate migration of BASP-1, α5-integrin, β1-integrin, and EGFR. White arrowheads indicate migration of p140. Of the tested species, only a band reactive with anti-α5-integrin comigrated with p140.

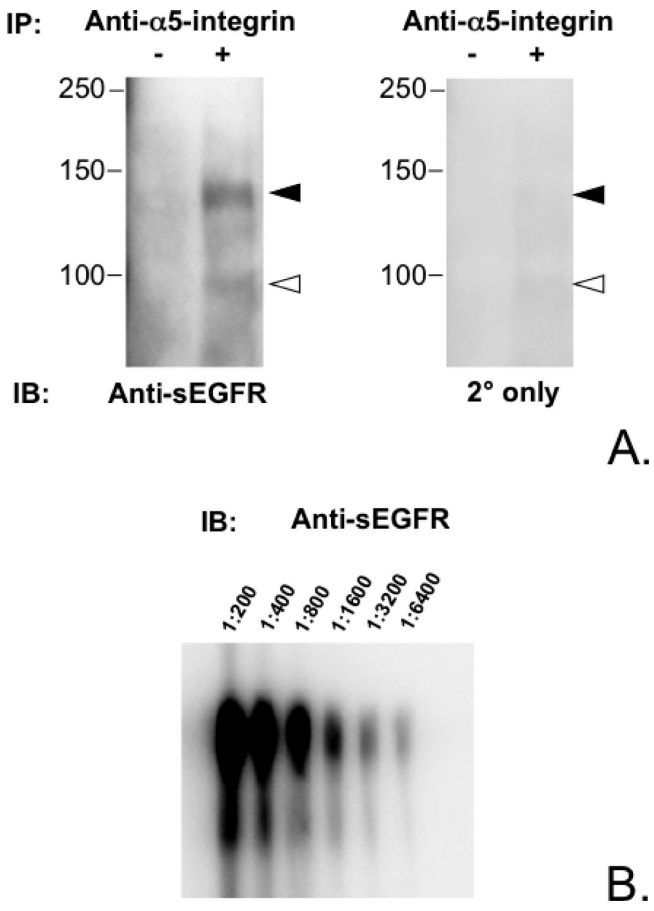

Figure 5. Anti-sEGFR recognizes α5-integrin. (A) Immunoblot of p140 immunoprecipitated from JEG-3 cell lysates with anti-α5-integrin antibody and reacted with anti-sEGFR (right) or secondary antibody alone (left). The black arrowheads indicate the mobility of p140. The white arrowheads indicate the mobility of a minor ~95 kDa band, which we postulate is a product of α5-integrin. (B) Immunoblot of recombinant α5/β1-integrin that reacted with different dilutions of anti-sEGFR, as indicated, confirming that anti-sEGFR recognizes α5-integrin.

a hydration chamber. The drops were incubated overnight at 37 °C, 5% CO_2, and 95% humidity, allowing cells to coalesce. Images were captured and analyzed using IP Lab imaging and analysis software. Each image was adjusted for optimum contrast. To measure aggregate size, outlines were automatically traced and the number of pixels within the outlines was calculated. Data points representing the mean and standard error for aggregate size expressed in pixels (a measure of aggregate compaction) were calculated from nine aggregates of each cell line. Aggregate size was compared by one-way ANOVA and Tukey's multiple-comparisons test. Because both CHO-P3 and CHO-α5 cells form circular sheets in the presence of anti-sEGFR, it was possible to calculate differences in surface area by converting pixel diameter to actual diameter and calculating area using standard equations. Statistical analysis in this case was performed using an unpaired Student's *t* test.

RESULTS

The Anti-sEGFR Polyclonal Antibody Recognizes Two Proteins. To evaluate the expression of EGFR and sEGFR in a panel of human carcinoma-derived cell lines, we resolved whole cell lysates via SDS−PAGE and processed them for immunoblot analysis using a commercial antibody directed against the EGFR intracellular domain or an affinity-purified anti-sEGFR 31-mer antibody previously generated and characterized by our laboratory.[10] CHO cells stably expressing EGFR or sEGFR were used as positive controls.[10] Several cell lines (i.e., JEG-3, ES-2, HEY, IGROV-1, and OVCAR-5) expressed full-length EGFR, and several cell lines (i.e., JEG-3, A2780, A2780 CP-R, ES-2, and OVCAR-8) expressed an immunoreactive band migrating at the same apparent molecular mass (~90 kDa) as sEGFR expressed exogenously in CHO cells (Figure 2). Unexpectedly, some carcinoma-derived cell lines (i.e., JEG-3, A2780, A2780 CP-R, ES-2, HEY, and IGROV-1) also expressed a higher-apparent molecular mass protein of ~140 kDa (i.e., "p140") that can react with anti-sEGFR. Notably, p140 is strongly expressed in the choriocarcinoma-derived JEG-3 and ovarian cystadenocarcinoma-derived HEY cell lines.

p140 and sEGFR Are Biochemically Distinct Species As Evidenced by Differential Detergent Solubility. To determine whether p140 is related to sEGFR, we first compared the biochemical characteristics of these two proteins. JEG-3 cells

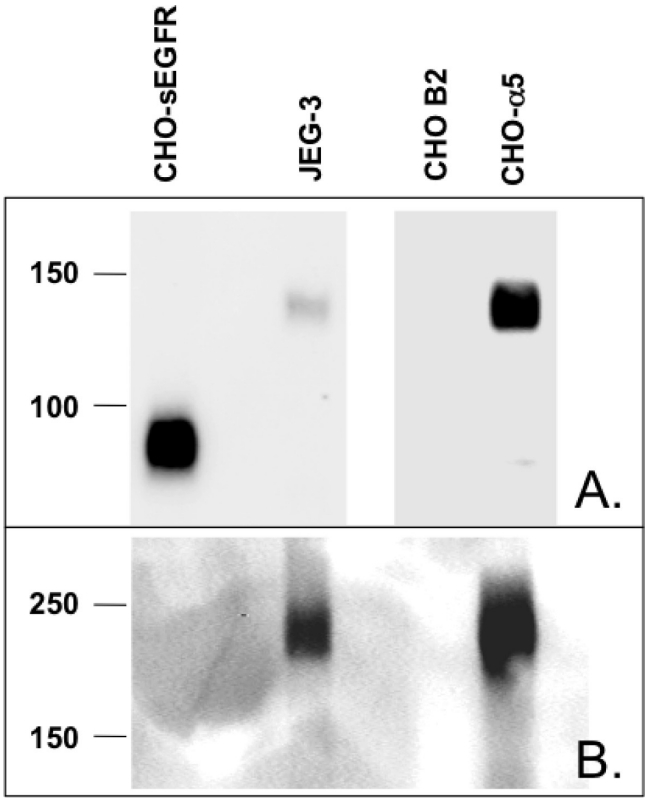

Figure 6. Expression of α5-integrin is detected by immunoblot analysis with anti-sEGFR and anti-α5-integrin antibodies. α5-Integrin deficient CHO-B2 cells express a very low level of endogenous α5-integrin as detected by anti-sEGFR (A) or anti-α5-integrin (B). Lysates of CHO-B2 cells stably expressing human α5-integrin (CHO-α5) contain species reactive as a band by reducing SDS−PAGE followed by anti-sEGFR immunoblot, or a higher-molecular mass band by nonreducing SDS−PAGE followed by anti-α5-integrin immunoblot (following the manufacturer's instructions for this antibody). CHO-sEGFR and JEG-3 cells are included as negative and positive controls for p140/α5-integrin, respectively. Note different exposure lengths for CHO-sEGFR and JEG-3 vs CHO-B2 and CHO-α5 in panel A for the sake of clarity.

were used for the purpose of purifying p140 because they express this protein in relative abundance (Figure 2). Cells were lysed to test the solubility of p140 versus sEGFR in various detergents and buffers (Figure S1 of the Supporting Information). JEG-3 cells lysed with an SDS/NP-40/DOC solution liberated both p140 and sEGFR into solution (Figure S1, lane 1). In contrast, JEG-3 cells lysed with buffer containing 1% TX-100 and 1 mM EDTA in PBS did not liberate p140 or sEGFR (Figure S1, lane 2). JEG-3 cells lysed with 0.5% DOC (Figure S1, lanes 3 and 6) or 2.5% SDS prepared without buffer or with TBS (Figure S1, lanes 4 and 7) also did not liberate p140. JEG-3 cells lysed with unbuffered 0.5% TX-100 (Figure S1, lane 5) but not with TX-100 buffered with TBS (Figure S1, lane 8) liberated p140 into solution. Additional experiments revealed that 1% TX-100 was the optimal concentration for solubilizing p140 from JEG-3 cell pellets in unbuffered solution and that 0.01% TX-100 was sufficient for maintaining p140 solubility (data not shown). In contrast, sEGFR was released with SDS (Figure S1, lane 4), but not with TX-100 (Figure S1, lane 5). This observation was the first indication that sEGFR and p140 were biochemically distinct membrane-associated proteins.

p140 Is α5-Integrin. To ascertain the identity of p140, we used conventional chromatographic methods to partially purify p140 from TX-100 JEG-3 lysates and then interrogated p140-enriched chromatography fractions via LC−ESI MS/MS. Purification of p140 was monitored by immunoblot analysis of chromatographic fractions with anti-sEGFR. We observed that p140 is efficiently depleted from JEG-3 lysates by SP Sepharose using binding buffers adjusted to pH ≤5.0; i.e., p140 binds strongly to SP Sepharose at pH ≤5.0, weakly between pH 5.5 and 6.5, and not at all at pH >7.0 (Figure 3A). Interestingly, most TX-100-solubilized proteins precipitate at pH 4.0 (by addition of 50 mM formic acid); however, p140 remains soluble, thus resulting in substantial p140 purification (data not shown). Consequently, we selected 50 mM formic acid (pH 4.0) as the binding buffer for SP Sepharose chromatography and NaCl as the eluant. Under these conditions, we observed that p140 elutes from SP Sepharose at ≥300 mM NaCl (Figure 3B). Additional studies demonstrated that p140 also binds to hydroxylapatite in 20 mM sodium phosphate buffer (pH 6.8) and elutes with 90−110 mM sodium phosphate (Figure 3C). The final purification protocol for subsequent LC−ESI MS/MS analysis thus consisted of extraction with TX-100 and formic acid followed by preparative chromatography with SP Sepharose and hydroxylapatite; fractions that eluted with 200−370 mM NaCl and 80−160 mM sodium phosphate were pooled. LC−ESI MS/MS analysis of p140-enriched chromatographic fractions identified peptides corresponding to α5-integrin, β1-integrin, and brain acid soluble protein-1 (BASP1/NAP-22/CAP-23), which exhibit apparent molecular masses of ∼140, ∼130, and ∼55 kDa, respectively, via SDS−PAGE (Table 1). Immunoblot analysis of JEG-3 and HEY cell lysates probed with antibodies specific for α5-integrin, β1-integrin, BASP-1, sEGFR, and EGFR detected proteins of ∼140, 130, 52, 140, and 170 kDa, respectively (Figure 4). Remarkably, p140 reacted with antibodies specific for both sEGFR and α5-integrin.

To confirm that p140 reacts with both anti-α5-integrin and anti-sEGFR, JEG-3 lysates were immunoprecipitated with an anti-α5-integrin antibody followed by immunoblot analysis with anti-sEGFR. As illustrated in Figure 5A, the anti-α5-integrin antibody immunoprecipitates a 140 kDa protein that is cross-reactive with anti-sEGFR. Furthermore, anti-sEGFR recognizes a commercial preparation of purified recombinant α5/β1 integrin (Figure 5B), but not purified recombinant αv/β3 integrin (Figure S2 of the Supporting Information). Additionally, as shown in Figure 6, a 140 kDa protein cross-reactive with anti-sEGFR can be detected in lysates of CHO cells engineered to express human α5-integrin (CHO-α5)[13] but is not observed in lysates of CHO parental cells that express only low levels of endogenous (hamster) α5-integrin (CHO-B2). Together with the identity of the p140 peptides presented in Table 1 (which correspond to α5-integrin), these immunoblot results demonstrate that p140 is α5-integrin, and also that α5-integrin harbors an epitope(s) that is immunoreactive with affinity-purified anti-sEGFR.

Anti-sEGFR Binds to Conserved Sequences in the Calf-1 Domain of α5-Integrin. To identify the epitope(s) of α5-integrin recognized by anti-sEGFR, we subjected α5-integrin to CNBr hydrolysis. Figure 7A demonstrates the predicted CNBr cleavage sites of α5-integrin. CNBr treatment of recombinant α5/β1-integrin yielded one major band of 27 kDa that is detected by anti-sEGFR using immunoblot analysis (Figure 8A). This reactive band was excised from the gel,

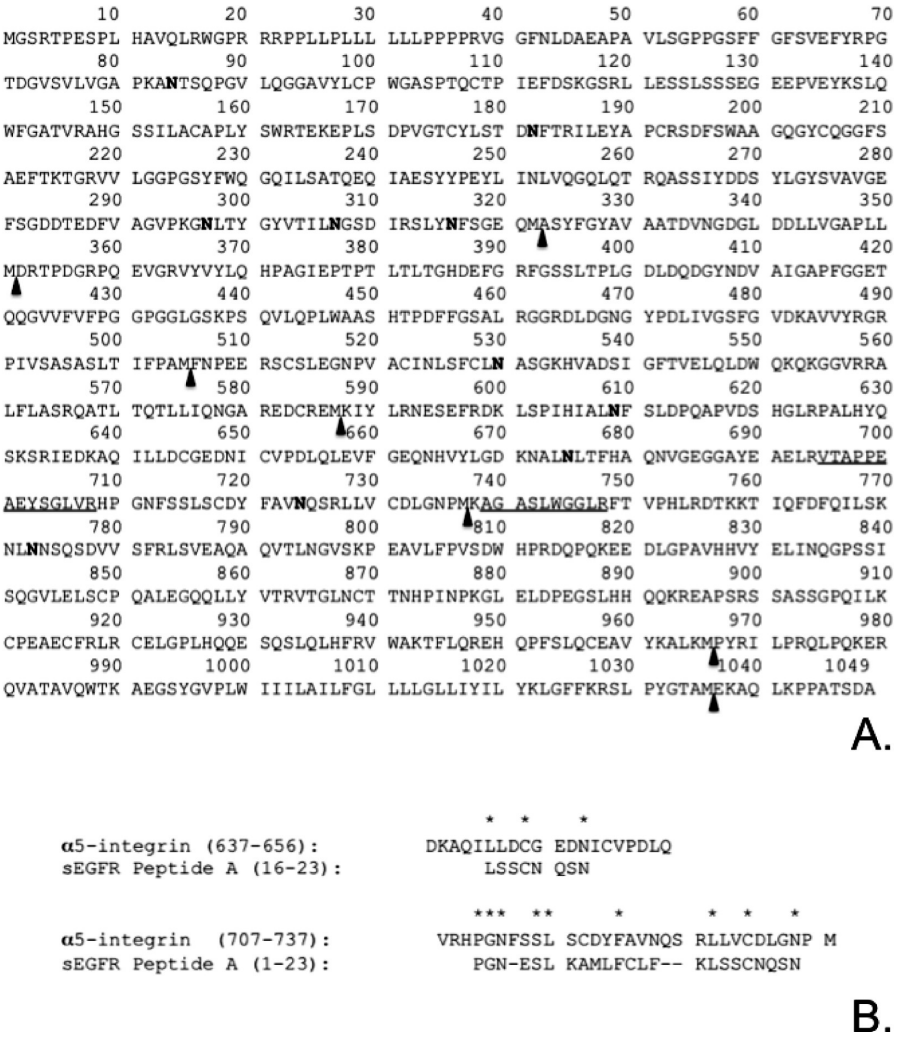

Figure 7. (A) Diagram of the α5-integrin amino acid sequence. Predicted sites of CNBr cleavage are denoted with arrowheads. Peptides recovered by LC−ESI MS/MS from an anti-sEGFR 31-mer immunoreactive 27 kDa gel band generated by CNBr hydrolysis are underlined: ^{695}VTAPPEAEYSGLVR^{708} and ^{739}AGASLWGGLR^{748}. Potential sites of N-linked glycosylation are highlighted in bold. Potential sites of cyanogen bromide cleavage are indicated with black arrowheads. (B) Sequence comparison of α5-integrin residues 588−737 with the sEGFR 31-mer peptide. Regions of α5-integrin that are >35% identical with sEGFR were aligned according to SIM analysis (http://www.expasy.org/tools/sim-prot.html). Amino acids sharing sequence identity are denoted with asterisks.

digested with trypsin, and analyzed by LC−ESI MS/MS, which identified two α5-integrin peptides: ^{695}VTAPPEAEYSGLVR^{708} and ^{739}AGASLWGGLR^{748} (Figure 7A, underlined). Conspicuously, peptides 695−708 and 739−748 reside on distinct CNBr cleavage products consisting of residues 588−737 and 738−966, respectively, thus restricting the location of the anti-sEGFR binding epitope to α5-integrin residues 588−966. On the basis of amino acid sequence inspection, peptides 588−737 and 738−966 have predicted molecular masses of ∼17 and ∼27 kDa, respectively. However, peptide 588−737 contains at least three potential sites of N-linked glycosylation, whereas peptide 738−966 contains only one potential glycosylation site (http://www.cbs.dtu.dk/services/NetNGlyc). Depending on the nature of the carbohydrate moiety or moieties involved, such glycosylation events could increase the observed molecular mobility of peptide 588−737 by as much as 9 kDa (based on a predicted ∼3 kDa per complex triantennary glycan). As such, peptide 588−737 is of the correct apparent molecular mass to correspond to a glycosylated, 27 kDa CNBr fragment of α5-integrin. To confirm the identity of the 27 kDa anti-sEGFR immunoreactive band as α5-integrin peptide 588−737 (vs 738−966), we treated recombinant α5/β1-integrin with PNGaseF, a pan-N-glycosidase, prior to CNBr hydrolysis. This combination treatment yielded a deglycosylated anti-sEGFR immunoreactive band of ∼17 kDa, the predicted deglycosylated mass of α5-integrin peptide 588−737 (Figure 8B), further restricting the location of the anti-sEGFR binding epitope(s).

The SIM alignment tool (http://www.expasy.ch/tools/sim-prot.html) was then used to compare the sEGFR 31-mer peptide to CNBr-cleaved α5-integrin peptide 588−737. Using 30% identity as the minimal cutoff threshold, two regions of sequence identity were identified between the sEGFR and α5-integrin peptides, further restricting the binding epitope(s) of anti-sEGFR. Notably, α5-integrin residues 710−735 (26-mer) and 642−649 (8-mer) are ∼35 and ∼38% identical with the 31-mer sEGFR peptide, respectively (Figure 7B), and both of these epitopes reside within α5-integrin's bioactive calf-1 domain.[19] To compare the binding of anti-sEGFR to its cognate 31-mer

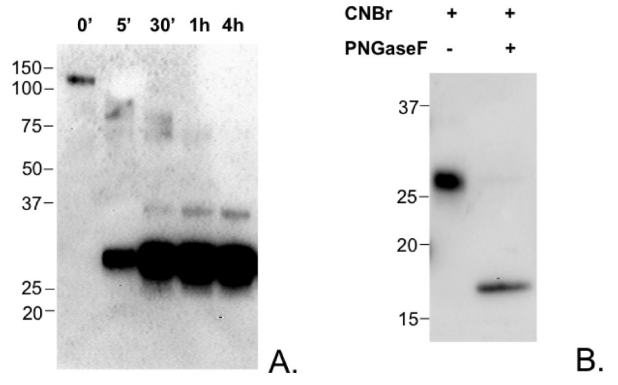

Figure 8. Immunoblots of recombinant α5/β-integrin digested by CNBr hydrolysis. (A) Time course of CNBr hydrolysis of recombinant α5/β1-integrin. CNBr hydrolysis was terminated at the times indicated. A precursor−product relationship is evident, resulting in an anti-sEGFR reactive band of ∼27 kDa. (B) CNBr hydrolysis of deglycosylated α5-integrin. Prior to CNBr hydrolysis, recombinant α5/β1-integrin was treated with PNGaseF. An anti-sEGFR reactive protein of ∼17 kDa was generated by this procedure; this peptide corresponds to α5-integrin peptide 588−737 (see Figure 7), indicating that the anti-sEGFR epitope of α5-integrin is located between amino acids 588 and 737.

immunogen versus the binding to these two α5-integrin peptides (note that residues 637−641 were included in peptide "642−649" to improve its solubility), all three peptides were analyzed by plasmon resonance in the presence of anti-sEGFR to determine their equilibrium binding constants (K_D). Sensorgrams illustrate that the level of binding of the antibody to the 31-mer sEGFR peptide is highest ($K_D = 6.34 \times 10^{-7}$ M) and exhibits a nonlinear relationship as predicted for a polyclonal antibody (Figure 9 and Table 2). In contrast, the anti-sEGFR binding affinities of α5-integrin peptides 637−649 ($K_D = 7.64 \times 10^{-6}$ M) and 710−735 ($K_D = 3.06 \times 10^{-6}$ M) are 12 and 5 times lower, respectively, than that observed for the 31-mer sEGFR peptide. In addition, peptides 637−649 and 710−73 have a linear binding relationship with anti-sEGFR that is consistent with the presence of a single immunoglobulin binding epitope in each of these two α5-integrin peptides. Interestingly, both of these putative anti-sEGFR binding sites are located within a critical regulatory region of α5-integrin termed the calf-1 domain.[19] A BLAST homology search reveals that the "LLDCGEDN" peptide (peptide 642−649) is perfectly repeated in only one other protein, αv-integrin; however, anti-sEGFR does not recognize αv-integrin by immunoblot analysis (Figure S2 of the Supporting Information). We conclude that there is a strong interaction between anti-sEGFR and α5-integrin in cell-free systems.

Anti-sEGFR Promotes Cell Compaction. The interaction between anti-sEGFR and α5-integrin raised the possibility that this antibody might influence cell surface integrin−ECM interactions. We previously have demonstrated an interaction between α5-integrin and its ligand, fibronectin, that regulates the intrinsic ability of cells to form intercellular connections, resulting in the formation of cohesive three-dimensional (3D) aggregates, in vitro.[17] Fibronectin is a secreted protein that has been shown, through direct interaction with α5-integrin, to promote such cell−cell interactions by playing a direct role in aggregate compaction.[13,14] We, therefore, hypothesized that anti-sEGFR might similarly regulate 3D assembly, thereby implicating the calf-1 domain in α5-integrin-mediated cell aggregation and tissue assembly.

To address this hypothesis, we evaluated the ability of anti-sEGFR to regulate 3D cell assembly using an aggregate compaction assay. Figure 10A illustrates several images of hanging drop cultures of CHO-P3 parental cells and CHO cells transfected to express α5-integrin (CHO-α5) captured after overnight incubation in PBS, rabbit IgG, or anti-sEGFR. In agreement with previous observations,[17] CHO-P3 parental cells (panel A) form loose, dispersed clusters, whereas CHO-α5 cells form tight, more compact clusters (panel B). The addition of rabbit IgG to either CHO-P3 (panel C) or CHO-α5 (panel D) cells had no effect on compaction. Addition of anti-sEGFR, however, resulted in markedly more compact aggregates of both CHO-P3 (panel E) and CHO-α5 (panel F) cells. However, the degree of anti-sEGFR-mediated compaction in CHO-α5 cells is much greater than that observed in parental CHO-P3 cells, suggesting pleiotropic regulation of tissue organization by anti-sEGFR in this in vitro model. Quantification and comparison of the aggregate size of each cell cluster using ANOVA and Tukey's multiple-comparisons test confirmed these effects of anti-sEGFR on compaction. Figure 10B shows that incubating CHO-α5 cells in anti-sEGFR gives rise to aggregates that are 50% smaller and more compact than those incubated in rabbit IgG ($p < 0.01$) or PBS ($p < 0.001$), whereas no difference in cluster size was evident between CHO-α5 cells incubated in PBS or rabbit IgG ($p > 0.05$). Moreover, α5-integrin-expressing CHO cells formed aggregates with a surface area of 0.0171 ± 0.0007 mm^2 when incubated in anti-sEGFR, whereas those of CHO-P3 incubated under the same conditions formed aggregates that were significantly larger with a surface area of 0.045 ± 0.001 mm^2 (Student's t test, $p < 0.0001$). Collectively, these data indicate that anti-sEGFR can regulate aggregate compaction and that this effect is markedly enhanced in α5-integrin-expressing cells. As discussed below, these observations may reveal a novel mechanism of α5-integrin-mediated cohesion transduced via its intrinsic calf-1 domain.

DISCUSSION

The role of EGFR in the etiology and progression of a variety of human cancers is well-established.[20] However, the utility of this receptor as a clinically useful biomarker has been limited by the considerable disparity that exists among published reports regarding "EGFR expression" in human tissues and tumors as determined by immunohistochemistry. For example, in ovarian cancer, more than 40 published studies have been conducted, and only half conclude that EGFR is an independent prognostic factor (reviewed in ref 21). We and others have proposed that this discordance can be attributed, at least in part, to the co-expression of sEGFR with EGFR in ovarian tumors.[22]

To develop immunological reagents that can distinguish between sEGFR and EGFR expression, we have generated a rabbit polyclonal antiserum directed against the unique carboxy-terminal sequence of sEGFR; this antiserum does not cross-react with full-length EGFR or other HER family receptors and is useful for the detection of sEGFR using immunoblot, immunoprecipitation, and immunohistochemical methods.[10] Initial characterization of this anti-sEGFR antibody using human carcinoma-derived cell lines revealed unexpected cross-reactivity with an unknown 140 kDa protein, which we here identify as human α5-integrin. This observation was unanticipated because previous BLAST searches indicated no significant homology between the unique sEGFR 78-amino acid carboxy-terminal sequence and any known protein.[5] Here we show that α5-

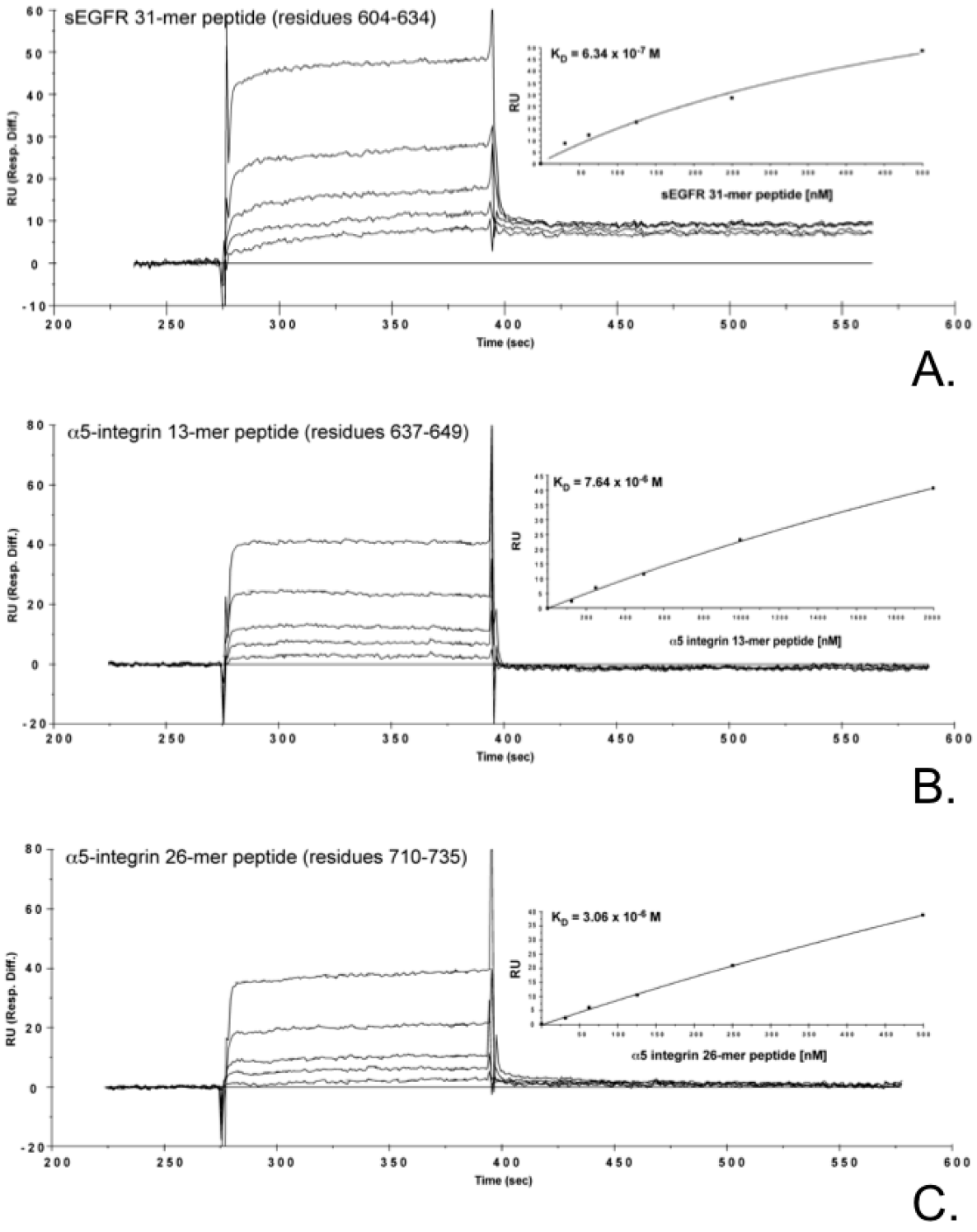

Figure 9. Surface plasmon resonance sensorgrams of anti-sEGFR binding to a sEGFR vs two α5-integrin peptides. Absorbance in relative units (RU) is plotted vs time (seconds) for immobilized anti-sEGFR in the presence of sEGFR 31-mer peptide 604−634 (A), α5-integrin peptide 637−649 (B), and α5-integrin peptide 710−735 (C). Graphs of RU vs peptide concentration are included as insets.

integrin harbors two immunoreactive epitopes that are 35% (26-mer) and 38% (8-mer) identical with the unique carboxy-terminal sequence of sEGFR. However, we demonstrate that only the 26-mer epitope of intact α5-integrin is immunoreactive with anti-sEGFR.

The significance of these observations is several-fold. First, these observations will inform the development of next-generation antibodies truly specific for either sEGFR or α5-integrin. Second, these results suggest that studies using anti-α5-integrin antibodies should be viewed cautiously until the specificity of such antibodies is empirically established, because sEGFR expression is ubiquitous in human tissues, including human blood. Identification of p140 as human α5-integrin was only possible through

Table 2. Summary of the Surface Plasmon Resonance of Interactions of sEGFR and α5-Integrin Peptide with Anti-sEGFR

peptide	amino acid sequence	anti-sEGFR antibody equilibrium binding constant (K_D) (M)
sEGFR 31-mer	PGNESLKAMLFCLFKL-SSCNQSNDGSVSHQS	6.34×10^{-7}
α5-integrin 637−649	DKAQILLDCGEDN	7.64×10^{-6}
α5-integrin 710−735	PGNFSSLSCDYFAVNQ-SRLLVCDLGN	3.06×10^{-6}

rigorous biochemical evaluation and could not have been predicted via typical sequence comparison algorithms. Finally, while the functional implications of these short regions of sequence homology between sEGFR and α5-integrin have not yet been fully determined, previous studies of antibody cross-reactivity among structurally divergent adhesion molecules suggest that such regions of structural identify may reflect aspects of shared functions that arise via convergent evolution.[23]

By analogy, we propose that the homologous regions reported here might have functional significance, perhaps providing contact regions characteristic of the homophillic and/or even homotypic interactions defined by other cell surface adhesion molecules. In support of this concept, we have shown that anti-sEGFR induces aggregation and compaction of suspended cells in culture, and that the ability of anti-sEGFR to induce cell compaction is correlated with the level of α5-integrin expression. While the mechanism underlying anti-sEGFR-induced 3D cell assembly is not yet known, it is possible that by analogy to our previous studies with fibronectin[13,14] anti-sEGFR activates α5-integrin by mediating its cross-linking, thereby promoting aggregation between CHO cells; alternatively, this antibody may inhibit cell sheet compaction in favor of higher-order coalescence (allowing for greater overall tissue spherical compaction). This newly identified function of an antibody directed against sEGFR, which also recognizes α5-integrin, is consistent with the emerging role of sHER3, a soluble isoform of the HER3 receptor, in prostate cancer cell adhesion and metastasis.[24,25] Given that serum sEGFR concentrations are dysregulated in diverse malignancies,[26] proteolysis of cell surface sEGFR also may regulate cell adhesion, proliferation, and/or migration responses in a manner paralleling proteolysis of homophilic cell−cell CAM complexes.[27] These studies, therefore, not only identify anti-sEGFR as a novel probe for future studies of integrin function but also specifically implicate the calf-1 domain of α5-integrin as a transducer of 3D tissue compaction and, possibly, cohesion.

In addition to the shared homology between α5-integrin and sEGFR, α5-integrin is a cell surface coreceptor (along with β1-integrin) for fibronectin, and in its ligated form, this complex acts in concert with full-length EGFR to promote EGF-independent cell survival signaling.[28−30] The precise nature of this cell surface protein complex has been studied extensively, but the role of sEGFR in the function of this complex has yet to be elucidated. The new findings presented here suggest a potential structural basis for such interactions and may provide a useful focus for future structure−function analyses. In particular, the calf-1 domain of α5-integrin is known to play a critical role in the conformational shift of integrin to its ligand binding state.[31]

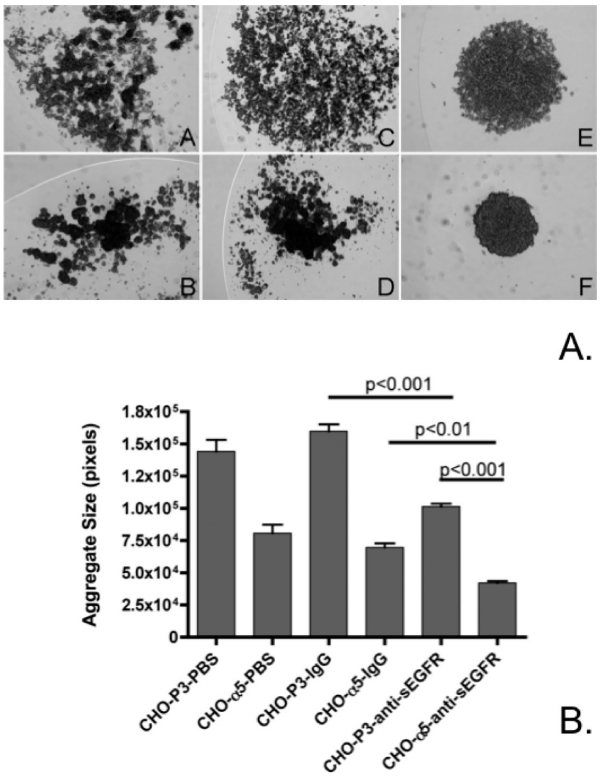

Figure 10. (A) Anti-sEGFR promotes compaction of suspended CHO-B2 cells. Compaction of CHO-P3 and CHO-α5 was compared by suspending cells in hanging drops in the presence of PBS (A and B), rabbit IgG (C and D), or anti-sEGFR (E and F). In general, anti-sEGFR appears to markedly enhance aggregate compaction. This effect is greater for α5-integrin-expressing cells than for control cell lines. (B) Quantification of aggregate size. Image analysis was used to calculate average aggregate size for parental and α5-integrin-expressing cells incubated in hanging drop cultures in PBS, rabbit IgG, and anti-sEGFR. Statistical analysis by ANOVA revealed a significant difference in aggregate size in response to anti-sEGFR treatment ($p < 0.0001$). Tukey's multiple-comparisons test revealed a pairwise difference between the following groups of cells: CHO-P3-anti-sEGFR and CHO-α5-anti-sEGFR ($p < 0.001$), CHO-α5-IgG and CHO-α5-anti-sEGFR ($p < 0.01$), and CHO-P3-IgG and CHO-P3-anti-sEGFR ($p < 0.001$). As expected, no difference in size was detected between CHO-P3 and CHO-P3-IgG ($p > 0.05$) or CHO-α5 and CHO-α5 IgG ($p > 0.05$).

These results may similarly provide an initial focus for structure−function analysis of the unique carboxy terminus of sEGFR, as well as for further mapping of the integrin−EGFR complex that mediates cell adhesion and survival signaling.

It is noteworthy that, while both α5/β1-integrin and αv/β1-integrin function as receptors for fibronectin, α5/β1-integrin but not αv/β1-integrin transduces survival signals following fibronectin ligation.[32] In this regard, α5-integrin expression has been correlated with progression-free and overall survival in ovarian cancer patients, although to date, α5-integrin has not been a reliable prognostic indicator in the clinic.[33] Moreover, α5β1-integrin-directed cancer therapeutics such as volociximab are in clinical trials for the treatment of patients with diverse solid tumors, including epithelial ovarian cancer, pancreatic cancer, and non-small cell lung cancer (clinicaltrials.gov identifiers NCT00635193, NCT00401570, and NCT00654758, respectively). The clear diagnostic and theragnostic potential of EGFR, sEGFR, and α5-integrin, therefore, not only underscores the

need for a more complete understanding of the functional attributes of these proteins, both alone and in complex, but also makes it imperative that the immunological reagents to be used for the clinical detection of these proteins be reliably monospecific.

In conclusion, we speculate that the short regions of limited sequence homology between sEGFR and α5-integrin identified here may be functionally and biologically significant. Moreover, the identification of an antibody that has the potential to detect both proteins with high affinity reveals the need for caution in interpreting either sEGFR or α5-integrin expression data that rely solely on immunohistochemical methods. The results presented here are consistent with recent studies that suggest that antibodies directed against various EGFR isoforms can exhibit unanticipated complexities, particularly in cancer cells,[34,35] and also that these complexities provide windows of opportunity for improving our understanding of the structure and function of these important growth regulatory proteins, as well as their clinical utility.

■ ASSOCIATED CONTENT

Supporting Information. Solubility of p140 in various buffers (Figure S1) and specificity of anti-sEGFR for α5-integrin (Figure S2). This material is available free of charge via the Internet at http://pubs.acs.org.

■ AUTHOR INFORMATION

Corresponding Author

*Yale School of Medicine, P.O. Box 208063, 310 Cedar St., New Haven, CT 06520-8063. Phone: (203) 623-5142. Fax: (203) 737-2914. E-mail: nita.maihle@yale.edu.

Funding Sources

This work was supported by grants from Susan G. Komen for the Cure and the Marsha Rivkin Center for Ovarian Cancer Research to J.A.W., the Kentucky Lung Cancer Research Program and Markey Cancer Center Translational Research grants to A.T.B., National Institutes of Health (NIH) Grant CA 118755 to R.A.F., NIH Grant CA 15083-35 to D.J.M., and NIH Grant CA 79808 and a "Senior Women in Medicine Professorship" from Yale University School of Medicine to N.J.M.

■ ACKNOWLEDGMENT

We thank Drs. Elliott Bedows (University of Nebraska Medical Center, Omaha, NE) and Nathan Vanderford (University of Kentucky) for their editorial assistance and critical review of the manuscript, Dr. Jack Goodman (University of Kentucky) for LC−ESI MS/MS technical assistance, Ms. Jane Peterson (Mayo Clinic) for synthesis and purification of synthetic peptides, Dr. Jun Hiyashi (Precision Antibody) for surface plasmon resonance technical assistance, and KJ Studio (www.kjstudio.com) for the graphic for the table of contents.

■ ABBREVIATIONS

BASP-1, brain acid soluble protein 1; BSA, bovine serum albumin; CHO, Chinese hamster ovary; CNBr, cyanogen bromide; DOC, deoxycholate; ECD, extracellular domain; ECL, enhanced chemiluminescence; EDTA, ethylenediaminetetraacetic acid; EGFR, epidermal growth factor receptor; FBS, fetal bovine serum; HER, human epidermal growth factor receptor; K-PBS, potassium phosphate-buffered saline; LC−ESI MS/MS, liquid chromatography and electrospray ionization tandem mass spectrometry; NFDM, nonfat dry milk; PAGE, polyacrylamide gel electrophoresis; PBS, phosphate buffered saline; PVDF, polyvinylidene difluoride; RU, relative units; SDS, sodium dodecyl sulfate; sEGFR, soluble epidermal growth factor receptor; TBS, Trizma-buffered saline; TBS-TW20, Trizma-buffered saline with 0.1% Tween 20; TFA, trifluoroacetic acid; TX-100, Triton X-100.

■ REFERENCES

(1) Yarden, Y., and Sliwkowski, M. X. (2001) Untangling the ErbB signalling network. *Nat. Rev. Mol. Cell Biol. 2*, 127–137.

(2) Boerner, J. L., Danielsen, A., and Maihle, N. J. (2003) Ligand-independent oncogenic signaling by the epidermal growth factor receptor: v-ErbB as a paradigm. *Exp. Cell Res. 284*, 111–121.

(3) Flynn, J. F., Wong, C., and Wu, J. M. (2009) Anti-EGFR Therapy: Mechanism and Advances in Clinical Efficacy in Breast Cancer. *J. Oncol. 2009*, 526963.

(4) Maihle, N. J., Baron, A. T., Barrette, B. A., Boardman, C. H., Christensen, T. A., Cora, E. M., Faupel-Badger, J. M., Greenwood, T., Juneja, S. C., Lafky, J. M., Lee, H., Reiter, J. L., and Podratz, K. C. (2002) EGF/ErbB receptor family in ovarian cancer. *Cancer Treat. Res. 107*, 247–258.

(5) Reiter, J. L., Threadgill, D. W., Eley, G. D., Strunk, K. E., Danielsen, A. J., Sinclair, C. S., Pearsall, R. S., Green, P. J., Yee, D., Lampland, A. L., Balasubramaniam, S., Crossley, T. D., Magnuson, T. R., James, C. D., and Maihle, N. J. (2001) Comparative genomic sequence analysis and isolation of human and mouse alternative EGFR transcripts encoding truncated receptor isoforms. *Genomics 71*, 1–20.

(6) Reiter, J. L., and Maihle, N. J. (2003) Characterization and expression of novel 60-kDa and 110-kDa EGFR isoforms in human placenta. *Ann. N.Y. Acad. Sci. 995*, 39–47.

(7) Baron, A. T., Cora, E. M., Lafky, J. M., Boardman, C. H., Buenafe, M. C., Rademaker, A., Liu, D., Fishman, D. A., Podratz, K. C., and Maihle, N. J. (2003) Soluble epidermal growth factor receptor (sEGFR/sErbB1) as a potential risk, screening, and diagnostic serum biomarker of epithelial ovarian cancer. *Cancer Epidemiol., Biomarkers Prev. 12*, 103–113.

(8) Leslie, K. K., Sill, M. W., Darcy, K. M., Baron, A. T., Wilken, J. A., Godwin, A. K., Cook, J., Schilder, R. J., Schilder, J. M., and Maihle, N. J. (2009) Efficacy and safety of gefitinib and potential prognostic value of soluble EGFR, EGFR mutations, and tumor markers in a Gynecologic Oncology Group phase II trial of persistent or recurrent endometrial cancer. *J. Clin. Oncol.27*, Abstract e16542.

(9) Lafky, J. M., Baron, A. T., Cora, E. M., Hillman, D. W., Suman, V. J., Perez, E. A., Ingle, J. N., and Maihle, N. J. (2005) Serum soluble epidermal growth factor receptor concentrations decrease in postmenopausal metastatic breast cancer patients treated with letrozole. *Cancer Res. 65*, 3059–3062.

(10) Christensen, T. A., Reiter, J. L., Baron, A. T., and Maihle, N. J. (2002) Generation and characterization of polyclonal antibodies specific for human p110 sEGFR. *Hybridoma Hybridomics 21*, 183–189.

(11) Xiong, J. P., Stehle, T., Zhang, R., Joachimiak, A., Frech, M., Goodman, S. L., and Arnaout, M. A. (2002) Crystal structure of the extracellular segment of integrin αVβ3 in complex with an Arg-Gly-Asp ligand. *Science 296*, 151–155.

(12) Schreiner, C. L., Bauer, J. S., Danilov, Y. N., Hussein, S., Sczekan, M. M., and Juliano, R. L. (1989) Isolation and characterization of Chinese hamster ovary cell variants deficient in the expression of fibronectin receptor. *J. Cell Biol. 109*, 3157–3167.

(13) Robinson, E. E., Zazzali, K. M., Corbett, S. A., and Foty, R. A. (2003) α5β1 integrin mediates strong tissue cohesion. *J. Cell Sci. 116*, 377–386.

(14) Robinson, E. E., Foty, R. A., and Corbett, S. A. (2004) Fibronectin matrix assembly regulates α5β1-mediated cell cohesion. *Mol. Biol. Cell 15*, 973–981.

(15) Myers, E. W., and Miller, W. (1988) Optimal alignments in linear space. *Comput. Appl. Biosci. 4*, 11–17.

(16) Brown, N. K., McCormick, D. J., David, C. S., and Kong, Y. C. (2008) H2E-derived Eα52−68 peptide presented by H2Ab interferes with clonal deletion of autoreactive T cells in autoimmune thyroiditis. *J. Immunol. 180*, 7039–7046.

(17) Caicedo-Carvajal, C. E., Shinbrot, T., and Foty, R. A. (2010) α5β1 integrin-fibronectin interactions specify liquid to solid phase transition of 3D cellular aggregates. *PLoS One 5*, e11830.

(18) Corbett, S. A., Lee, L., Wilson, C. L., and Schwarzbauer, J. E. (1997) Covalent cross-linking of fibronectin to fibrin is required for maximal cell adhesion to a fibronectin-fibrin matrix. *J. Biol. Chem. 272*, 24999–25005.

(19) Kamata, T., Handa, M., Sato, Y., Ikeda, Y., and Aiso, S. (2005) Membrane-proximal α/β stalk interactions differentially regulate integrin activation. *J. Biol. Chem. 280*, 24775–24783.

(20) Uberall, I., Kolar, Z., Trojanec, R., Berkovcova, J., and Hajduch, M. (2008) The status and role of ErbB receptors in human cancer. *Exp. Mol. Pathol. 84*, 79–89.

(21) Lafky, J. M., Wilken, J. A., Baron, A. T., and Maihle, N. J. (2008) Clinical implications of the ErbB/epidermal growth factor (EGF) receptor family and its ligands in ovarian cancer. *Biochim. Biophys. Acta 1785*, 232–265.

(22) Wilken, J. A., Baron, A. T., and Maihle, N. J. (2010) The epidermal growth factor receptor conundrum. *Cancer*.

(23) Grumet, M., Hoffman, S., and Edelman, G. M. (1984) Two antigenically related neuronal cell adhesion molecules of different specificities mediate neuron-neuron and neuron-glia adhesion. *Proc. Natl. Acad. Sci. U.S.A. 81*, 267–271.

(24) Vakar-Lopez, F., Cheng, C. J., Kim, J., Shi, G. G., Troncoso, P., Tu, S. M., Yu-Lee, L. Y., and Lin, S. H. (2004) Up-regulation of MDA-BF-1, a secreted isoform of ErbB3, in metastatic prostate cancer cells and activated osteoblasts in bone marrow. *J. Pathol. 203*, 688–695.

(25) Chen, N., Ye, X. C., Chu, K., Navone, N. M., Sage, E. H., Yu-Lee, L. Y., Logothetis, C. J., and Lin, S. H. (2007) A secreted isoform of ErbB3 promotes osteonectin expression in bone and enhances the invasiveness of prostate cancer cells. *Cancer Res. 67*, 6544–6548.

(26) Baron, A. T., Wilken, J. A., Haggstrom, D. E., Goodrich, S. T., and Maihle, N. J. (2009) Clinical implementation of soluble EGFR (sEGFR) as a theragnostic serum biomarker of breast, lung and ovarian cancer. *IDrugs 12*, 302–308.

(27) Craig, S. E., and Brady-Kalnay, S. M. (2011) Cancer cells cut homophilic cell adhesion molecules and run. *Cancer Res. 71*, 303–309.

(28) Liu, D., Aguirre Ghiso, J., Estrada, Y., and Ossowski, L. (2002) EGFR is a transducer of the urokinase receptor initiated signal that is required for in vivo growth of a human carcinoma. *Cancer Cell 1*, 445–457.

(29) Ingber, D. E. (2006) Cellular mechanotransduction: Putting all the pieces together again. *FASEB J. 20*, 811–827.

(30) Wang, F., Weaver, V. M., Petersen, O. W., Larabell, C. A., Dedhar, S., Briand, P., Lupu, R., and Bissell, M. J. (1998) Reciprocal interactions between β1-integrin and epidermal growth factor receptor in three-dimensional basement membrane breast cultures: A different perspective in epithelial biology. *Proc. Natl. Acad. Sci. U.S.A. 95*, 14821–14826.

(31) Clark, K., Pankov, R., Travis, M. A., Askari, J. A., Mould, A. P., Craig, S. E., Newham, P., Yamada, K. M., and Humphries, M. J. (2005) A specific α5β1-integrin conformation promotes directional integrin translocation and fibronectin matrix formation. *J. Cell Sci. 118*, 291–300.

(32) Zhang, Z., Vuori, K., Reed, J. C., and Ruoslahti, E. (1995) The α5β1 integrin supports survival of cells on fibronectin and up-regulates Bcl-2 expression. *Proc. Natl. Acad. Sci. U.S.A. 92*, 6161–6165.

(33) Sawada, K., Mitra, A. K., Radjabi, A. R., Bhaskar, V., Kistner, E. O., Tretiakova, M., Jagadeeswaran, S., Montag, A., Becker, A., Kenny, H. A., Peter, M. E., Ramakrishnan, V., Yamada, S. D., and Lengyel, E. (2008) Loss of E-cadherin promotes ovarian cancer metastasis via α5-integrin, which is a therapeutic target. *Cancer Res. 68*, 2329–2339.

(34) Garrett, T. P., Burgess, A. W., Gan, H. K., Luwor, R. B., Cartwright, G., Walker, F., Orchard, S. G., Clayton, A. H., Nice, E. C., Rothacker, J., Catimel, B., Cavenee, W. K., Old, L. J., Stockert, E., Ritter, G., Adams, T. E., Hoyne, P. A., Wittrup, D., Chao, G., Cochran, J. R., Luo, C., Lou, M., Huyton, T., Xu, Y., Fairlie, W. D., Yao, S., Scott, A. M., and Johns, T. G. (2009) Antibodies specifically targeting a locally misfolded region of tumor associated EGFR. *Proc. Natl. Acad. Sci. U.S.A. 106*, 5082–5087.

(35) Swami, M. (2009) Immunotherapy: A hidden target. *Nat. Rev. Cancer 9*, 318–319.

(36) Sato, Y., Isaji, T., Tajiri, M., Yoshida-Yamamoto, S., Yoshinaka, T., Somehara, T., Fukuda, T., Wada, Y., and Gu, J. (2009) An N-glycosylation site on the β-propeller domain of the integrin α5 subunit plays key roles in both its function and site-specific modification by β1,4-N-acetylglucosaminyltransferase III. *J. Biol. Chem. 284*, 11873–11881.

(37) Mosevitsky, M. I., Capony, J. P., Skladchikova, G., Novitskaya, V. A., Plekhanov, A., and Zakharov, V. V. (1997) The BASP1 family of myristoylated proteins abundant in axonal termini. Primary structure analysis and physico-chemical properties. *Biochimie 79*, 373–384.